ELSEVIER

International Journal of Mass Spectrometry 205 (2001) 43–55

Electron energy loss and dissociative electron attachment spectroscopy of methyl vinyl ether and related compounds

C. Bulliard[a], M. Allan[a,*], S. Grimme[b]

[a]*Institut de Chimie Physique, Université de Fribourg, Pérolles, CH-1700 Fribourg, Switzerland*
[b]*Organisch-Chemisches Institut der Universität Münster, Corrensstrasse 40, D-48149 Münster, Germany*

Received 10 February 2000; accepted 11 April 2000

Abstract

The triplet and singlet excited states of methyl vinyl ether have been characterized by electron energy loss spectroscopy and multireference density functional theory with configuration interaction (DFT/MRCI). The electron attachment energy was determined from the excitation functions for vibrational excitation to be 2.3 eV. Dissociative electron attachment spectra have been measured with a mass spectrometer having a trochoidal monochromator in the incident electron beam. Fragment anion bands peaking at 3 eV, 6.5 eV and 9.5 eV have been found in methyl vinyl ether. The first band is assigned to the $^2(\pi^*)$ shape resonance, the second band to a resonance where an electron is loosely bound by dipole and polarization forces to the target molecule in its valence excited $^1(\pi, \pi^*)$ state, and the third band to Feshbach resonances with occupation of Rydberg orbitals. CH_3O^- and H_2CC^- are formed at 3 eV, CH_3O^- and HCC^- at 6.5 and 9.5 eV. The fragmentation pattern of ethyl vinyl ether at 3 eV is similar, yielding ethanolate and vinylidene anions, but with the unexpected addition of the deprotonated acetaldehyde anion CH_2CHO^-. The fragmentation patterns of methyl allyl ether and benzyl methyl ether are dominated by the methanolate anions with high intensity, indicating that dissociation of C–O bond in unsaturated ethers is much faster if this bond does not lie in the plane of the π system. (Int J Mass Spectrom 205 (2001) 43–55) © 2001 Elsevier Science B.V.

1. Introduction

The interest in electron-impact induced chemistry in general and in dissociative electron attachment (DA) in particular is being revived by the increasing importance of technological applications of low-pressure plasmas. The studies of electron-molecule scattering have greatly benefited from the invention of the trochoidal electron energy analyser by Stamatović in 1968 [1,2]. It has been far superior to the retarding potential difference (RPD) method commonly used at that time and has immediately become indispensable for the DA [3] and the electron transmission spectroscopy (ETS) [4] techniques. A full electron energy-loss spectrometer based on this principle, that is an instrument using trochoidal energy selectors not only to prepare the incident electron beam, but also to energy-analyse inelastically scattered electrons, has proven to be more difficult to built. Early efforts have been hampered by the fact that the primary electron beam is injected directly into the energy analyser in the coaxial geometry required by the magnetic field. It is many orders of magnitude more intense than the inelastically scattered electrons that one attempts to

* Corresponding author. E-mail: michael.allan@unifr.ch

Dedicated to Professor Aleksandar Stamatovic on the occasion of his 60th birthday.

PII S1387-3806(00)00283-9

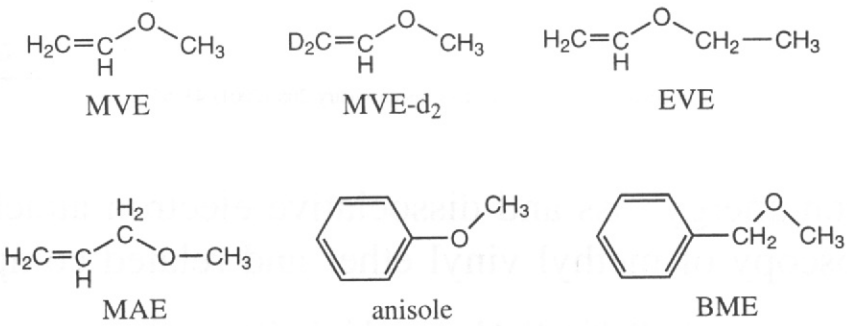

Scheme 1.

detect and causes a large background of stray electrons. The Yale group did prove the feasibility of a such an instrument [5], however.

The use of trochoidal electron monochromators has had a long tradition in Fribourg. One of us (MA) has been fortunate to learn how to build and use these devices in the laboratory where they were invented and to enjoy direct instruction by A. Stamatović during his visits to Yale. The electron energy-loss spectrometer based on trochoidal monochromators has been improved in Fribourg, mainly by the use of two trochoidal analysers in series, which dramatically reduced the amount of stray electrons [6]. An instrument for the study of DA was constructed in Fribourg soon thereafter [7].

Trochoidal monochromators are superior to electrostatic energy selectors in several aspects. Their transmission function is more stable at low energies, they positively reject the (unwanted) fragment anions, generally provide more intense electron beams and are simple and less expensive to construct. They have been built and used in many institutions, the list of which would be too long to be included here, particularly in ETS and DA instruments. The full electron energy-loss spectrometers based on throchoidal spectrometers have also been constructed in several, albeit much fewer places around the world, in the groups of Jordan [8], Shpenik, [9,10], and Belić [11,12]. Cloutier and Sanche have developed a trochoidal electron spectrometer for the study of surfaces [13]. In spite of all this effort, Stamatović has remained unsurpassed in the art of tuning his own invention to the highest resolution [14–16].

Three techniques using trochoidal monochromators are used in the present work. Anionic fragmentation processes of methyl vinyl ether (MVE) have been studied using the dissociative electron attachment spectroscopy. The interpretation of the fragmentation patterns is facilitated by the knowledge of the triplet and singlet excited states of neutral MVE, which have been determined with the electron energy loss spectroscopy. And finally the negative ion resonances have been measured using the electron transmission spectroscopy and the cross sections for vibrational and electronic excitation. The assignment of the excited states of MVE is based on multireference density functional calculations with configuration interaction (DFT/MRCI). The results are complemented by a DA study of ethyl vinyl ether (EVE), methyl allyl ether (MAE), anisole, and benzyl methyl ether (BME) (Scheme 1).

2. Experiment

The trochoidal electron spectrometer used in the present study has been described in more detail in the literature [6,17,18]. It uses a trochoidal monochromator to prepare a quasimonoenergetic electron beam and two trochoidal analysers in series to select the energy of the scattered electrons. The electrons collide with a quasi-static gas sample in a collision chamber. Both forward- and backward-scattered electrons are detected [17,18], although the pulsed beam scheme to separate them was not used in the present

work. The excitation functions are corrected for the response function of the energy analyser.

The DA spectrometer has been described elsewhere [7,19,20]. A trochoidal monochromator is employed to generate a beam of electrons with narrow energy distribution. It collides with sample gas in a target chamber, fragment anions are extracted at 90°, and detected after passing a quadrupole mass filter. The energy scale was calibrated on the O^-/CO_2 signal, by placing the energy of a point at 50% of the first peak height to the theoretical onset at 3.998 eV. Energy resolution was about 0.12 eV, as determined from the width of the onset of the O^-/CO_2 signal (difference of energies of points at 25% and 75% of peak height).

An important part of the present results are the fragment appearance energies, given by the onsets of the observed signal. Their determination from the spectra is complicated by the fact that the observed bands are broadened by the instrumental profile and by hot bands, whose intensity can be enhanced to a degree which we do not know when the DA cross section rises with vibrational excitation of the target. At which point of the observed band should the onset be taken is thus not obvious and depends on the inherent shape of the band, which is not directly accessible. If the inherent signal were a very narrow peak, then the energy of the peak of the observed signal should be taken. If the inherent signal were a step function at threshold, then the energy at 50% of peak height should be taken. If the inherent signal rises gradually, then the energy at less than 50% of the peak height should be taken. The fragment ion bands that we observe are generally substantially wider than the instrumental resolution, indicating that the first limiting case is not appropriate. The low-energy side of the observed fragment ion signal with the present compounds is steep, but more gradual than the observed onset of the O^-/CO_2 signal (which is inherently vertical). This indicates that the inherent signal onsets encountered in this study are steep, but not vertical. The gradual onsets are presumably caused in part by hot bands (sample temperature was about 60°). But the cross sections are very probably also inherently gradually increasing due to an increasing number of final channels, corresponding to vibrationally excited fragments, with increasing energy above threshold. In view of these problems we have decided to adopt a pragmatic and conservative approach, by taking the onset at 50% of the observed peak height and allowing for the above uncertainties by taking an error bar of about the same magnitude as the observed width of the signal onsets, that is ±0.2 eV.

The background pressure in the instrument was around 10^{-6} mbar. The sample pressure in the target chamber has not been measured, but is estimated to be of the order of 10^{-3} mbar. The path of the fragment ions in the target chamber is short (2.5 mm), reducing the possibility of reactions of the fragment ions with the sample molecules in secondary collisions. We thus feel confident that the observed signals are not due to secondary collisions.

MVE-d_2 was prepared in three steps from methoxyacetate and lithium aluminium deuteride [20,21]. The remaining compounds are commercial samples.

3. Theory

All DFT calculations have been performed with the TURBOMOLE suite of programs [22,23]. The ground state of MVE is fully optimized in C_s symmetry employing the B3LYP exchange correlation functional [24,25]. Valence triple-ζ Gaussian AO basis sets augmented with polarization functions on all atoms ([5s3p1d]/[3s1p] [26]) are used. The *cis*-structure considered is found to be more stable by 2.0 kcal/mol than the *trans*-conformer. The DFT/MRCI calculations are performed as described in detail elsewhere [27] using the BHLYP [28] functional which ensures a proper description of the asymptotic form of the potential far away from the nuclei which is important for a description of Rydbergs states. In these calculations the AO basis is augmented by one set of diffuse sp-functions on each nonhydrogen atom. With an energy cutoff value of 1.0 E_h about 2×10^4 configuration state functions (CSF) are selected for the lowest eight states in each symmetry. The number

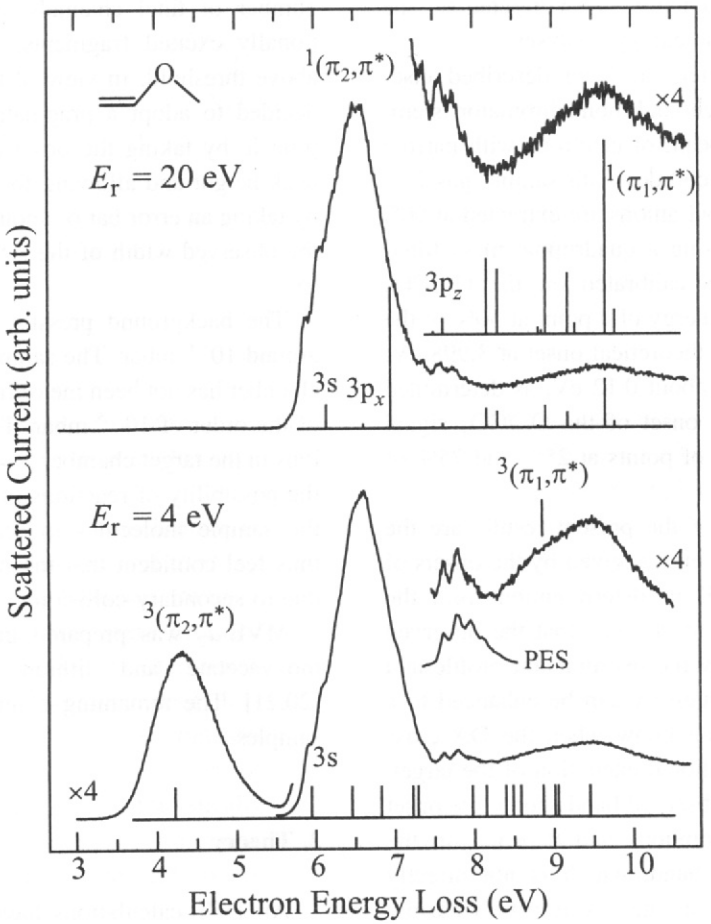

Fig. 1. Electron energy loss spectra of MVE, compared to the singlet (top) and triplet (bottom) transition energies calculated with the DFT/MRCI method. The profile of the first PES band (horizontally shifted) is shown below the expanded section of the lower curve to emphasize the similarity of the PES and Rydberg band shapes.

of reference configurations is 58 in both the singlet and triplet calculations. The oscillator strengths (f) are obtained from the dipole-lengths form.

4. Results and discussion

4.1. Electron energy loss spectra

The EELS spectrum recorded at a residual energy of 20 eV and shown in the upper part of Fig. 1 is representative for the dipole and spin allowed transitions. It compares well with the photoabsorption spectrum of Planckaert et al. [29]. The assignment of the transitions is based on comparison (both in terms of transition energies and band intensities) with the results of a DFT/MRCI calculation, shown graphically in Fig. 1 and listed together with the measured transition energies in Table 1. The weak shoulders on the left side of the most intense band are assigned to transitions to the singlet 3s Rydberg state. The intense band itself is assigned to the valence $\pi_2 \rightarrow \pi^*$ transition. It is calculated 0.48 eV too high, more than the typical error of a DFT/MRCI calculation (the rms error for a wide range of molecules is ~0.2 eV [27]), presumably because of the complexity of calculating a valence state mixing with several Rydberg states, a

Table 1
Excitation energies of MVE[a]

Singlets					
ΔE_{EELS}	ΔE_{UV}	$\Delta E_{DFT/MRCI}$	1000 f	$\Delta\langle r^2\rangle$	assignment
5.88 (0_0^0)	5.87	6.15	72	30	3s
		6.62	12	29	$3p_x$
6.48 (vert.)	6.60	6.96	428	11	$\pi_2 \rightarrow \pi^*$
7.05 (0_0^0 ?)	7.04	6.98	1	35	$3p_y$
		7.50	2	35	$3d_{x^2-y^2}$
7.59 (0_0^0)	7.57	7.62	12	28	$3p_z$
		8.17	58	37	$3d_{xy}$
		8.31	49	34	$3d_{z^2}$
		8.82	5	12	$\sigma \rightarrow \pi^*$ + Ryd.
		8.86	3	14	$\sigma \rightarrow \pi^*$ + Ryd.
		8.91	66	33	$3d_{xz}$
		9.19	47	29	$3d_{yz}$
		9.28	8	26	$\sigma \rightarrow 3s$
9.6 (vert.)		9.66	148	9	$\pi_1 \rightarrow \pi^*$
Triplets					
ΔE_{EELS}	—	$\Delta E_{DFT/MRCI}$	—	$\Delta\langle r^2\rangle$	assignment
4.20 (vert.)		4.22		1	$\pi_2 \rightarrow \pi^*$
		5.95		29	$\pi_2 \rightarrow 3s$
		8.49		3	$\sigma \rightarrow \pi^*$
8.8 (vert.)		8.87		18	$\pi_1 \rightarrow \pi^*$ + Ryd.

[a] The photoabsorption values ΔE_{UV} are taken from Ref. [29]. $\Delta\langle r^2\rangle$ indicates the change of the $\langle r^2\rangle$ expectation value of the excited state with respect to that of the ground state, that is the increase of the spatial size of the electronic wave function upon excitation. The $\langle r^2\rangle$ expectation value of the ground state is 56 a_0^2. The occupied π orbitals are labeled π_1 and π_2 (essentially the in-phase and out-of-phase combinations of the π_{C-C} and p_π on oxygen), π^* designates the normally unoccupied π MO. The x-axis is taken approximately along the C—C bond, the y-axis is in the C—C—O plane. Rydberg transitions originate in the π_2 MO except where otherwise noted. Triplet Rydberg states above 6 eV are not listed for brevity.

problem known already for ethene. Weak undulation may be discerned on the top of the valence band and on its right flank (seen also in the spectrum with E_r = 4 eV), and are presumably due to transitions to the $3p_x$ and $3p_y$ states. (Table 1 gives the energy of the first discernable structure at 7.05 eV, it is not certain, however, whether it is the (0_0^0) peak. Planckaert et al. [29] put the origin at an energy lower by one quantum of the C=C stretch vibration.) The more pronounced vibrational structure in the 7.5–8.0 eV range is assigned as a transition to the $3p_z$ state. The Rydberg nature of this state is born out by the similarity of the band shape with that of the photoelectron spectrum (PES) [20,29,30]. (Our assignment of these peaks differs from that of Planckaert et al. [29], who suggested 3d.) Several relatively intense 3d Rydberg transitions are calculated in the 8.0–9.2 eV range, but do not lead to resolved vibrational structure in the spectrum. The broad band peaking at 9.6 eV is assigned to the second valence $\pi \rightarrow \pi^*$ transition.

The triplet $\pi_2 \rightarrow \pi^*$ transition is seen clearly at 4.2 eV in the lower spectrum of Fig. 1. The very good agreement between theory and experiment in this case (ΔE(calc.) = 4.22 eV) indicates that the problems with the singlet $\pi_2 \rightarrow \pi^*$ valence state indeed has a physical reason (i.e., strong vibrationally induced R–V mixing). The remainder of the spectrum recorded at E_r = 4 eV resembles the upper spectrum and thus does not reveal more triplet states, except that the 9.6 eV band has a broad shoulder around 8.8 eV which can be assigned to the triplet $\pi_1 \rightarrow \pi^*$ transition calculated at 8.87 eV, albeit mixed with other valence and Rydberg transitions (Table 1).

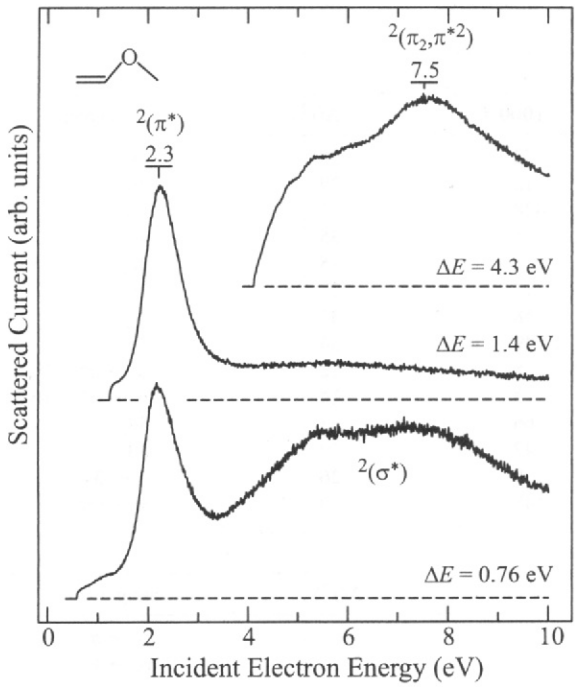

Fig. 2. Excitation functions for two energy losses corresponding to pure vibrational excitation and for the excitation of the lowest triplet state of MVE. (the weak undulation on the signal below 6 eV in the topmost spectrum is due to the 'focusing' artefact).

4.2. Excitation functions

Bands in the excitation functions for vibrational energy losses generally indicate shape resonances [31], which may alternatively be called temporary negative ions (TNI). Figure 2 shows excitation functions for the energy losses of 0.76 eV, corresponding to the excitation of two quanta of the (unresolved) C—H stretch vibrations, and 1.4 eV, which also includes vibrations other than C—H stretch. The results follow the pattern found for many organic compounds [17].

The band at 2.3 eV (also seen in ETS [20]) can be assigned as the $^2(\pi^*)$ shape resonance. The $^2(\pi^*)$ shape resonance of ethene is at 1.8 eV [32] so that the temporarily occupied π^* orbital of MVE can be viewed as essentially the C=C π^* orbital, conjugatively destabilized by an admixture of the p_π orbital of the oxygen atom. The very broad bands in the 5–8 eV range in the C—H excitation can be assigned to $^2(\sigma^*)$ shape resonances.

The excitation function of the $^3(\pi_2, \pi^*)$ triplet state of MVE shown at the top of Fig. 2 resembles that of the $^3(\pi, \pi^*)$ state of ethene [33]. In analogy to ethene we assign the signal from threshold to 6 eV as a tail of the $^2(\pi^*)$ resonance, and the band at 7.5 eV as a $^2(\pi_2, \pi^*2)$ core excited shape resonance, with a double occupation of the π^* MO, and the $^3(\pi_2, \pi^*)$ triplet state of MVE as a parent state. (Here the word *core* means the neutral molecule left behind when the *extra* electron is formally removed from the resonance—in contrast to the common usage in quantum chemistry, where it means the 1s atomic orbitals.)

4.3. Dissociative electron attachment to MVE

The yields of the two most prominent negative ion fragments are shown in function of the incident electron energy in Fig. 3. The bands around 3 eV can be assigned to dissociation following capture of the electron into the π^* MO. The DA bands peak at energies slightly higher than those of the resonance itself (Fig. 2), indicating that they are cut off by the thermochemical threshold on the left.

The 6.60 eV band in the yield of the fragment with m/e = 31 coincides in energy and in shape with the $^1(\pi_2, \pi^*)$ excited state (Fig. 1). DA bands which coincide with the lowest singlet valence excited state of the neutral molecule are found quite frequently, for example in CS_2 [34], and a number of other compounds [35], including dihalosubstituted toluenes [36] and possibly even ozone [37]. They have been assigned as $^2(\pi, \pi^*s)$ states, that is, as consisting of an electron in a diffuse s-wave function, loosely bound by dipole and polarisation potential of the parent excited $^1(\pi, \pi^*)$ state. The phenomenon is not entirely understood, however: it is not clear why these resonant states are pronounced in the dissociative attachment spectra, but not visible in other decay channels. It is not clear why no such resonant states are associated with the triplet excited states of the target.

The bands in the 8–10 eV range are generally assigned to Feshbach resonances with occupation of Rydberg orbitals [38].

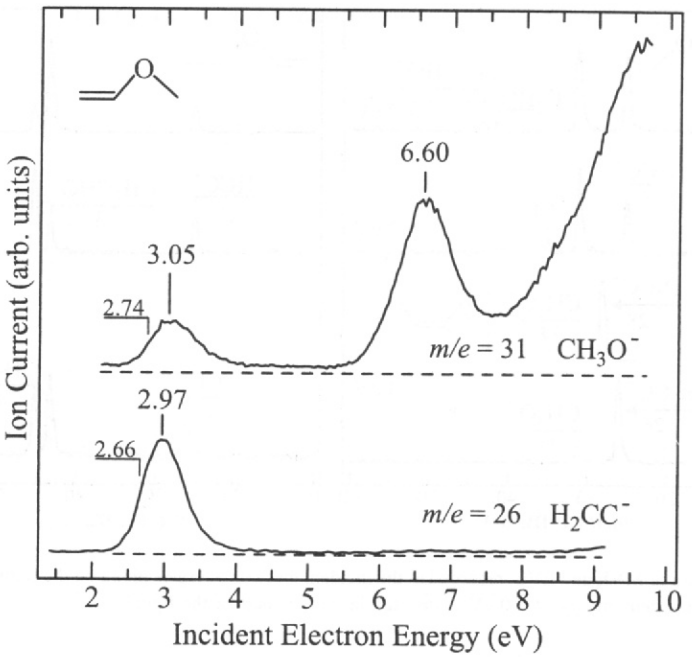

Fig. 3. Negative ion yields from MVE.

The present discussion focuses on the low-lying bands, where the fact that only few dissociation channels are open permits more definite conclusions about the dissociation mechanism. The observation of CH_3O^- [reaction (1)] is not surprising in view of the relatively large electron affinity of CH_3O (1.57 ± 0.02 eV [39]) and the fact that only one bond has to be broken. The experimental onset (accurate within ±0.2 eV, taken at 50% of peak height, see section 2), is 2.74 eV, in agreement with the threshold enthalpy [40] of 2.77 ± 0.2 eV. (ΔH_f^0 of MVE is taken as 1.09 eV [the mean value of Ref. 41–44]).

$$D_2C{=}C(H){-}O{-}CH_3 + e^- \quad (1)$$

$$\longrightarrow D_2C{=}CH + CH_3O^-$$

$$\longrightarrow D_2C{=}C^- + CH_3OH \quad (2)$$

$$\not\longrightarrow D{-}C{\equiv}C{-}H + CH_3OD \quad (3)$$

The onset of the $H_2C{=}C^-$ signal is at 2.66 eV, far below the thermochemical threshold enthalpy [40] for the formation of $H_2C{=}C^-$, CH_3O and H (7.55 eV). This indicates that the more stable neutral fragment CH_3OH is formed [reaction (2)], for which the thermochemical threshold enthalpy is calculated to be $\Delta H_f^0 = 3.02 \pm 0.2$ eV. Even this value is somewhat high, on the edge of the combined error limits of the present experiment and the thermochemical data. The difference could indicate that the ΔH_f^0 assumed for H_2CC^- (387 ± 15 kJ/mol [40]) could be too high by 0.36 eV (34 kJ/mol).

Two bonds must be broken and one made in the formation of CH_3OH. This relatively complicated rearrangement could occur in a concerted way, or CH_3O^- could be formed in a first step, but remain temporarily attached to the vinyl radical in an ion-molecule complex, a proton transfer would then lead to the observed products. The observation of the vinylidene anion is quite remarkable either way, because H_2CC^- was found to quantitatively abstract protons from CH_3OH in flowing afterglow experi-

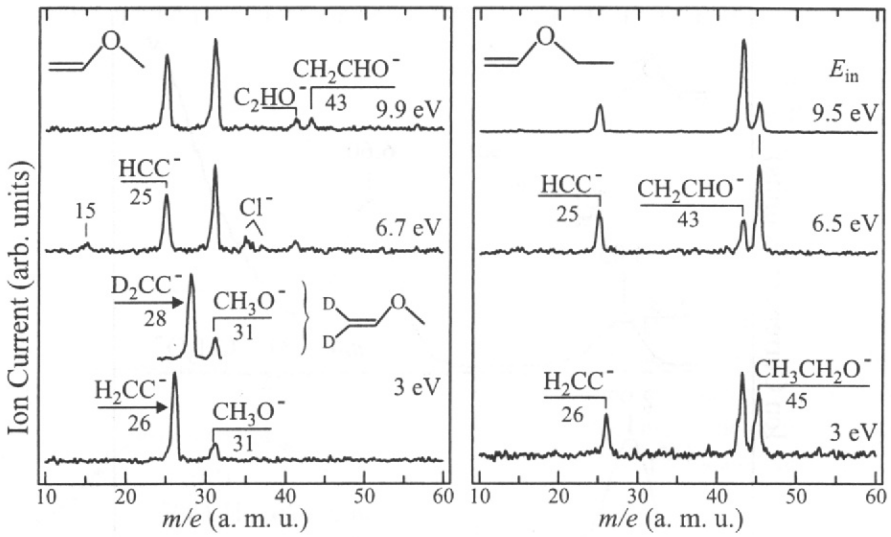

Fig. 4. Negative ion mass spectra of MVE and EVE, recorded at the incident electron energies given on the right of each frame. Mass spectrum of MVE-d_2 recorded with an incident energy of 3.0 eV is inserted in the left part of the figure.

ments, that is vinyl radical has been determined to be less acidic than methanol [45].

DA spectra of MVE-d_2 show only fragments with mass 28 (vinylidene anion-d_2 D_2CC^-) and no mass 27 ($DC{=}CH^-$), that is only the product of proton abstraction from the α and not from the β carbon atom [20] (Fig. 4). (The shapes of the curves showing the yields of the m/e = 38 and m/e = 31 fragments from MVE-d_2 in function of the electron energy are nearly identical to those of the m/e = 26 and m/e = 31 fragments from MVE [20].) This observation could be an indication of a concerted reaction path, but does not exclude an intermediate ion-molecule complex by itself. In that case the proton transfer could be very fast and not allow the CH_3O^- to travel to the β carbon atom. Abstraction of a proton on the β carbon atom would lead to a bent acetylene anion, as in reaction (3). MP2 calculations with large basis set indicate that vinylidene anion and *trans* bent acetylene anion are about equally stable [46], a more recent calculation predicts the *trans* bent acetylene anion to be more stable by 0.12 eV [47]. The formation of vinylidene anion and *trans* bent acetylene anion should thus have about the same threshold energy—and be energetically possible. It is not certain, however, that a *trans* bent acetylene anion would be observed in a mass spectrometer. The vertical attachment energy of linear acetylene is 2.6 eV [32], linear acetylene is autodetaching. It is strongly stabilized by bending [46,49,47], however, whereas neutral acetylene is destabilized, so that *trans* bent acetylene anion could be metastable in a way similar to the metastable bent CO_2^- [48]. *Trans* bent acetylene anion is stable in frozen matrices [49,50]. On the other hand a MP2 calculation led to the conclusion that even *trans* bent acetylene anion is autodetaching in the gas phase [46].

It is interesting that the 6.6 eV and ~9 eV bands are nearly absent in the yield of the $H_2C{=}C^-$ fragment.

4.4. Related compounds

The mass spectrum of EVE is compared to that of MVE in Fig. 4. The spectra of the two compounds have many analogies. The $CH_3CH_2O^-$ fragment analogous to the CH_3O^- fragment of MVE) and the $H_2C{=}C^-$ fragment are observed [reactions (4) and (5)]. The yields of these fragments in function of the incident electron energy are very similar in the two compounds (Fig. 5). A band peaking near 3.0 eV is

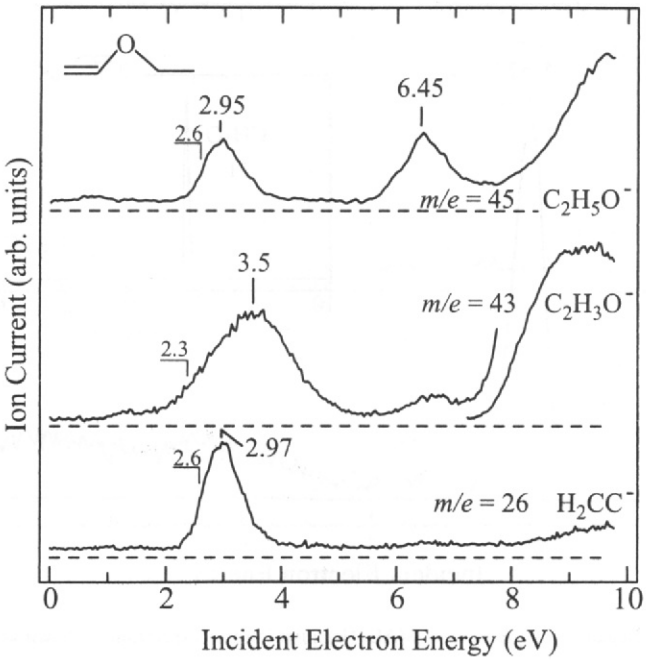

Fig. 5. Negative ion yields from EVE.

found for both, additional bands at 6.45 eV and ~9 eV are found for $CH_3CH_2O^-$. There is, however, a difference in the relative intensities of the vinylidene and alkoxy anion fragments: ethoxy is more intense relative to vinylidene in EVE than methoxy in MVE. The relatively higher yield of the ethoxy anion could be a consequence of its weaker basicity compared to methoxy anion (the acidities of ethanol and methanol are 1583 ± 4 kJ/mol and 1596 ± 1.7 kJ/mol, respectively [40]).

$$H_2C{=}CH{-}O{-}CH_2CH_3 + e^- \rightarrow H_2C{=}CH + CH_3CH_2O^- \quad (4)$$

$$\rightarrow H_2C{=}C^- + CH_3CH_2OH \quad (5)$$

$$\rightarrow H_2C{=}CHO^- + H + H_2C{=}CH_2 \quad (6)$$

The second striking difference is the fragment with mass 43 (deprotonated acetaldehyde), formed already at low energies. The yield of this fragment in dependence on the incident electron energy has a very weak shoulder with an onset at about 1.1 eV, followed by a much stronger band with an onset at about 2.3 eV and a gradual rise towards a peak at 3.5 eV. An obvious mechanism of its formation may seem to be breaking of the O—CH_2 bond, the loss of the ethyl group, with threshold enthalpy of 0.97 ± 0.1 eV [40]. The weak shoulder around 1 eV in the yield of the mass 43 in Fig. 5 could be due to this mechanism. The intense 3.5 eV band is not due to this simple mechanism, however, because one would then expect an analogous loss of a methyl group from MVE, which is not observed.

As an alternative we propose that the neutral products are H-atom and ethene, as in reaction (6), with a threshold enthalpy of 2.5 eV [40]. For the mechanism we propose that the EVE^- TNI first looses a H-atom in a first rapid step. The anion is thus stabilized and looses ethene in a second, slower step. If H-atom in the α position of the vinyl group is lost in the first step, then a hydrogen shift in a cyclic intermediate could lead to loss of ethene. The loss of H-atom from the vinyl group is forbidden, however, (they are located in the nodal plane of the π^* MO),

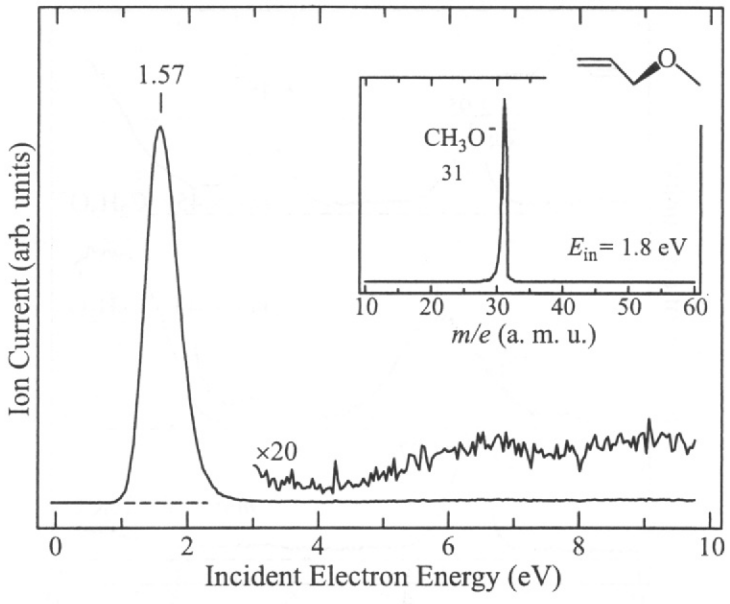

Fig. 6. Negative ion yields from MAE. Negative ion mass spectrum is shown as insert.

and we therefore find it more likely that a H-atom from the methylene group is lost first. A hydrogen shift from the β to the α position of the ethyl group would then be required for loss of ethene.

The experimental onset of the $CH_3CH_2O^-$ signal is at 2.6 eV, which is in agreement with the threshold enthalpy [40] of 2.64 ± 0.12 eV. The onset of the $H_2C{=}C^-$ signal from EVE is at 2.6 eV. The thermochemical threshold enthalpy [40], taking CH_3CH_2OH as the neutral fragment, is $\Delta H_f^0 = 3.02 \pm 0.2$ eV, the same as from MVE. Similar discrepancy (0.42 eV) between threshold enthalpy and observed onset is therefore found as for MVE. The discrepancy could be resolved by assuming $\Delta H_f^0 = 350 \pm 20$ kJ/mol for H_2CC^-.

The loss of the methoxy anion from MVE is to some degree analogous to the loss of halogen anion from vinyl chloride: it is symmetry forbidden. We therefore decided to test whether the yield of the methoxy anion from MAE, where the C—O bond being broken is rotated out from the plane of the $H_2C{=}CH^-$ moiety permitting direct conjugation of the π^* orbital where the incident electron is captured and the σ^* orbital of the C—O bond being broken, is enhanced in the same way as the yield of Cl^- from allyl chloride [51,52].

The spectra shown in Fig. 6 show that it is the case, they are dominated by an intense signal of the CH_3O^- fragment at low energies. The observed onset is in good agreement with the thermochemical threshold enthalpy of 1.32 eV.

Finally we tested whether the enhancement of the CH_3O^- fragment yield is also found in the anisole/BME pair. The BME spectra shown in Fig. 7 are very similar to those of MAE, they are entirely dominated by the CH_3O^- fragment at low energies. The anisole spectra on the other hand show no detectable anion fragment signal at low energies at all [20].

5. Conclusions

Apart from the known $^1(\pi_2, \pi^*)$ state and several Rydberg states, the DFT/MRCI calculation permitted the identification of the higher-lying $^1(\pi_1, \pi^*)$ state in MVE. The $^3(\pi_2, \pi^*)$ state is observed with low

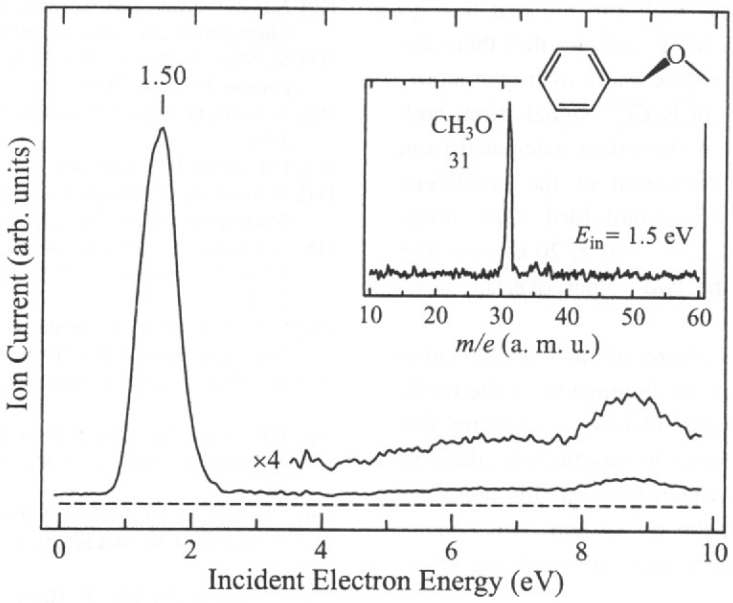

Fig. 7. Negative ion yields from BME. Negative ion mass spectrum is shown as insert.

residual energies. Excitation functions of vibrational energy losses and the $^3(\pi_2, \pi^*)$ state revealed a $^2(\pi^*)$ shape resonance at 2.3 eV, a broad band of $^2(\sigma^*)$ shape resonances in the 4–9 eV range, and a core excited shape resonance at 7.5 eV.

Standard thermochemical data predict the lowest dissociation threshold in MVE to be ~1 eV, leading to H_2CCHO^- (deprotonated acetaldehyde) and CH_3. No such signal is observed at MVE (and only a very weak signal is observed ~1 eV in EVE). Bands in the fragment anion yield have been observed at higher energies, peaking around 3 eV, 6.6 eV and 9.5 eV. The first band is assigned to the $^2(\pi^*)$ shape resonance, and the methanolate and vinylidene anions are formed. The formation of the methanolate anion is symmetry forbidden, but appears to proceed, albeit with an intensity much lower than that found in MAE, in a way similar to the formation of Cl^- from vinyl chloride. The formation of vinylidene anion at 3 eV requires that methanol is the neutral fragment. The vinylidene anion formation is somewhat puzzling in view of the observation in flowing afterglow that methanol reacts quantitatively with vinylidene anion to produce methanolate anion and vinyl radical [45]. Spectra of MVE-d_2 show only the dideutero vinylidene anion D_2CC^- and no monodeutero bent acetylene anion $DCCH^-$. This can be explained either by a concerted or nearly concerted formation of methanol, in which only the closest hydrogen participates, or, even if a deuteron were abstracted by an initially formed methanolate anion in a longer-lived methanolate-vinyl radical complex, the resulting *trans* bent acetylene anion would autodetach an electron and not reach the mass spectrometer.

The 6.6 eV band in MVE is assigned to a resonance where an electron is loosely bound by dipole and polarization forces to the target molecule in its valence excited $^1(\pi, \pi^*)$ state, the 9.5 eV band to Feshbach resonances with occupation of Rydberg orbitals. The dissociation is selective, vinylidene anion is not formed at the 6.6 and 9.5 eV bands.

The fragmentation pattern of EVE at 3 eV is similar to that of MVE, yielding ethanolate and vinylidene anions, but with the unexpected addition of the deprotonated acetaldehyde anion CH_2CHO^-, whose formation peaks at 3.5 eV. The relatively

high-lying onset of this band, and the fact that no analogy is observed in MVE indicate that there are two neutral fragments, ethene and a hydrogen atom.

The observed onsets of H_2CC^- signals from both MVE and EVE are below the values calculated from the literature heat of formation of the vinylidene anion, $\Delta H_f^0 = 380 \pm 15$ kJ/mol [40]. Our onsets would favor the value $\Delta H_f^0 = 350 \pm 20$ kJ/mol (The confidence ranges of the two values overlap, however.)

The fragmentation patterns of methyl allyl ether and benzyl methyl ether are dominated by the methanolate anions with high intensity, indicating that dissociation of C—O bond in unsaturated ethers is, for symmetry reasons, much faster if this bond lies outside of the plane of the π—system. This conclusion parallels that made in the corresponding unsaturated halides [51,52].

Acknowledgements

We express our sincere appreciation to professor Haselbach for his encouragement and support in the course of the present work. The experimental part of this study could not have been realized without the exceptionally qualified and enthusiastic work of M. Brosi of the mechanical shop and P.-H. Chassot of the electronic shop. The dideuterated ether has been prepared by Alexandre Robatel. This research is part of project No. 20-53568.98 of the Swiss National Science Foundation.

References

[1] A. Stamatović, G.J. Schulz, Rev. Sci. Instrum. 39 (1968) 1752.
[2] A. Stamatović, G.J. Schulz, Rev. Sci. Instrum. 41 (1970) 423.
[3] A. Stamatović, G.J. Schulz, Phys. Rev. A7 (1973) 589.
[4] L. Sanche, G.J. Schulz, Phys. Rev. A6 (1972) 69.
[5] W.C. Tam, S.F. Wong, Rev. Sci. Instrum. 50 (1979) 302.
[6] M. Allan, Helv. Chim. Acta 65 (1982) 2008.
[7] R.A. Dressler, M. Allan, Chem. Phys. 92 (1985) 449.
[8] D.E. Love, D. Nachtigallove, K.D. Jordan, J.M. Lawson, M.N. Paddon-Row, J. Am. Chem. Soc. 118 (1996) 1235.
[9] M.I. Romanyuk, O.B. Shpenik, Meas. Sci. Technol. 5 (1994) 239.
[10] N.I. Romanyuk, O.B. Shpenik, I.A. Mandu, F.F. Pann, I.V. Chernyshova, Zh. Tekh. Fiz. 63 (1993) 138 (in Russian).
[11] M. Vicić, G. Poparić, D.S. Belić, J. Phys. B 29 (1996) 1273; erratum 29 (1996) 2645.
[12] M. Vicić, G. Poparić, D.S. Belić, Rev. Sci. Instrum. 69 (1998) 1996.
[13] P. Cloutier, L. Sanche, Rev. Sci. Instrum. 60 (1989) 1054.
[14] S. Matejcik, A. Kiendler, A. Stamatović, T.D. Märk, Int. J. Mass Spectrom. Ion Processes 149/150 (1995) 311.
[15] P. Cicman, G. Senn, G. Denifl, D. Muigg, J.D. Skalny, P. Likac, A. Stamatović, T.D. Märk, Czech. J. Phys. 48 (1998) 1135.
[16] G. Senn, D. Muigg, G. Denifl, A. Stamatović, P. Scheier, T.D. Märk, Eur. Phys. J. D 9 (1999) 159.
[17] M. Allan, J. Electron Spectrosc. Relat. Phenom. 48 (1989) 219.
[18] K.R. Asmis, M. Allan, J. Phys. B 30 (1997) 1961.
[19] Y. Pariat, M. Allan, Int. J. Mass Spectr. Ion Proc. 103 (1991) 181.
[20] Ch. Bulliard, Ph.D. thesis, Fribourg 1994.
[21] F. Tureček, F.W. McLafferty, J. Am. Chem. Soc. 106 (1984) 2528.
[22] R. Ahlrichs, M. Bär, M. Häser, H. Horn, C. Kölmel, Chem. Phys. Lett. 162 (1989) 165.
[23] O. Treutler, R. Ahlrichs, J. Chem. Phys. 102 (1995) 346.
[24] A.D. Becke, J. Chem. Phys. 98 (1993) 5648.
[25] P.J. Stephens, F.J. Devlin, C.F. Chabalowski, M.J. Frisch, J. Phys. Chem. 98 (1994) 11623.
[26] A. Schäfer, C. Huber, R. Ahlrichs, J. Chem. Phys. 100 (1994) 5829.
[27] S. Grimme, M. Waletzke, J. Chem. Phys. 111 (1999) 5645.
[28] A.D. Becke, J. Chem. Phys. 98 (1993) 1372.
[29] A.A. Planckaert, J. Doucet, C. Sandorfy, J. Chem. Phys. 60 (1974) 4846.
[30] H. Bock, G. Wagner, K. Wittel, J. Sauer, D. Seebach, Chem. Ber. 107 (1974) 1869.
[31] G.J. Schulz, Rev. Mod. Phys. 45 (1973) 423.
[32] K.D. Jordan, P.D. Burrow, Acc. Chem. Res. 11 (1978) 341.
[33] M. Allan, Chem. Phys. Lett. 225 (1994) 156.
[34] R. Dressler, M. Allan, M. Tronc, J. Phys. B 20 (1987) 393.
[35] V.I. Khvostenko, A.S. Vorob'yov, O.G. Khvostenko, J. Phys. B 23 (1990) 1975.
[36] C. Bulliard, M. Allan, E. Haselbach, J. Phys. Chem. 98 (1994) 11040.
[37] M. Allan, K. Asmis, D. Popović, M. Stepanović, N.J. Mason, J.A. Davies, J. Phys. B 29 (1996) 4727.
[38] M.B. Robin, Higher Excited States of Polyatomic Molecules, Vol. 3, Academic Press, Orlando, 1985.
[39] P.C. Engleking, G.B. Ellison, W.C. Lineberger, J. Chem. Phys. 69 (1978) 1826.
[40] NIST Standard Reference Database. Available at: http://webbook.nist.gov/chemistry/.
[41] D.J. McAdoo, J.C. Traeger, C.E. Hudson, L.L. Griffin, J. Phys. Chem. 92 (1988) 1524.
[42] G. Frenking, N. Heinrich, J. Schmidt, H. Schwarz, Z. Naturforsch. 37b (1982) 1597.
[43] F.R. Cruickshank, S.W. Benson, J. Am. Chem. Soc. 91 (1969) 2487.

[44] S.G. Lias, J.E. Bartmess, J.F. Liebman, J.L. Holmes, R.D. Levin, W.G. Mallard, J. Phys. Chem. Ref. Data 17 (1988) 867.
[45] Y. Guo, J.J. Grabowski, Int. J. Mass Spectr. Ion Proc. 97 (1990) 253.
[46] J. Chandrasekhar, R.A. Kahn, P.R. Schleyer, Chem. Phys. Lett. 85 (1982) 493.
[47] S.B. Jursic, Int. J. Quantum Chem. 72 (1999) 571.
[48] C.D. Cooper, R.N. Compton, Chem. Phys. Lett. 14 (1972) 29.
[49] T. Kusumori, K. Matsuura, H. Muto, J. Chem. Phys. 104 (1996) 8879.
[50] Y. Itagaki, M. Shiotani, J. Phys. Chem. 103 (1999) 5189.
[51] R.A. Dressler, M. Allan, E. Haselbach, Chimia 39 (1985), 385.
[52] K.L. Stricklett, S.C. Chu, P.D. Burrow, Chem. Phys. Lett. 131 (1986) 279.